Evidence for a subtle structural symmetry breaking in EuB_6

2009 J. Phys.: Condens. Matter 21 456007

(http://iopscience.iop.org/0953-8984/21/45/456007)

J. Phys.: Condens. Matter **21** (2009) 456007 (5pp) doi:10.1088/0953-8984/21/45/456007

Evidence for a subtle structural symmetry breaking in EuB_6

H Martinho[1], C Rettori[2], G M Dalpian[1], J L F da Silva[3], Z Fisk[4] and S B Oseroff[5,6]

[1] Centro de Ciências Naturais e Humanas, Universidade Federal do ABC, Rua Santa Adélia 166, 09210-170, Santo André, São Paulo, Brazil
[2] Instituto de Física 'Gleb Wataghin', UNICAMP, 13083-970, Campinas, São Paulo, Brazil
[3] National Renewable Energy Laboratory, Golden, CO 80401, USA
[4] Department of Physics, University of California, Davis, CA 95616, USA
[5] San Diego State University, San Diego, CA 92182, USA
[6] Instituto de Ciencias Basicas, Universidad Nacional de Cuyo, Mendoza, Argentina

E-mail: herculano.martinho@ufabc.edu.br

Received 8 August 2009, in final form 22 September 2009
Published 23 October 2009
Online at stacks.iop.org/JPhysCM/21/456007

Abstract
This work presents a systematic Raman scattering study and first-principles calculations for the EuB_6 system. Evidence for the presence of an incipient ($\sim 1\times10^{-4}$ Å) tetragonal symmetry break of its crystalline structure was found. Forbidden Raman modes at $\omega_{\mathrm{fRm}(1)} \sim 1170\ \mathrm{cm}^{-1}$, $\omega_{\mathrm{fRm}(2)} \sim 1400\ \mathrm{cm}^{-1}$, and $\omega_{\mathrm{fRm}(3)} \sim 1500\ \mathrm{cm}^{-1}$ were observed. The tetragonal symmetry of $\omega_{\mathrm{fRm}(2)}$ and $\omega_{\mathrm{fRm}(3)}$ together with spin-polarized first-principles simulations of the structural and magnetic properties fully support such a break of symmetry. Our data and calculations explain the occurrence of ferromagnetism in Eu hexaborides, previously reported.

1. Introduction

The hexaborides RB_6 (R = alkaline-earth metal) are one of the most intensively studied groups of intermetallic compounds due to their large variety of physical ground states [1]. In particular, the family $R_{1-x}A_xB_6$ (A = magnetic rare earth) has attracted considerable interest due to the intriguing connections between their magnetic [2], transport [3], and optical properties [4, 5]. The available crystallographic data indicate that these compounds are cubic with the unit cell belonging to the O_h space group ($a \approx 4.19$ Å) [6]. The divalent alkaline metal occupies the central position on a cube, surrounded by eight B_6 octahedra, at each vertex [6].

EuB_6 is a ferromagnetic (FM) metal, characterized by a quite small effective carrier density at high T ($\sim 10^{-3}$ per unit cell) [7–11, 3, 12]. Actually, the physical processes occurring below $T \lesssim 16$ K are a matter of debate. Süllow *et al* [7] have shown that EuB_6 presents a FM transition at $T_{C1} = 15.3$ K where the spins order parallel to the [100] direction. A drop of an order of magnitude in its resistivity was also observed at this temperature and magnetic polaron overlap had been invoked to account for these features [8]. Andreev reflection spectroscopy combined with Hall effect and magnetoresistivity data indicated that EuB_6 has a semimetallic band structure with a fully spin-polarized hole band and an unpolarized electron band [9]. Eu-derived conduction band splitting due to coupling to core electrons at each Eu site was found to be the origin of the phase transition at T_{C1} [10]. The intimate correlation between magnetism and transport properties is believed to originate from the strong exchange interaction among spins of charge carriers and local f electrons [8]. At $T_{C2} = 12.5$ K spins undergo a reorientation transition to the [111] direction [7]. Below T_{C2} all Eu^{2+} spins participate in the long-range FM order [7, 13, 14]. Ferromagnetism in this case was found to arise from the half-filled 4f shell of Eu^{2+} ions, whose localized spins account for the measured magnetic moment of $\sim 7\ \mu_B$/f.u. [7, 11, 3].

Evidence for the occurrence of these two magnetic transitions below $T \lesssim 16$ K was found from muon spin rotation microscopic measurements by Brooks *et al* [15]. They concluded that the ferromagnetic state of EuB_6 is reached via two magnetic transitions at 15.5 K and 12.6 K, respectively. Two distinct components were resolved in the muon data, one oscillatory and one non-oscillatory, which arose from different kinds of magnetic environments [15].

The transition temperatures decrease with Ca content [3, 16] and are completely suppressed for $x \lesssim 0.30$ [17]. Electron microscopy data indicate the coexistence of insulating Ca-rich and metallic Eu-rich regions that percolate at $x \approx 0.30$ [17]. Moreover, Urbano *et al* [18] recently analyzed the behavior of the Eu^{2+} electron spin resonance (ESR) linewidth and concluded that the percolation of the impurity bound states has already started at $x \approx 0.15$, i.e., involving next to nearest neighbors.

The intriguing fact concerning EuB_6 is that symmetry constraints prevent the occurrence of FM order in the cubic O_h space group [19, 7]. Lattice symmetry must be lowered to one of the O_h tetragonal subgroups to allow ferromagnetism [7, 19]. High resolution T-dependent x-ray diffraction measurements by Süllow *et al* [7] failed to observe direct evidence of this symmetry breaking. However, they had observed an anisotropic intensity distribution of the Bragg peaks in all hl, hk, and kl planes that presented four symmetrically arranged wings around each peak. Strain at the sample surface, lattice disorder, vacancies or an incipient structural distortion were enumerated as possible origins for the wings but were not conclusively assigned. ESR g-value measurements on the $Ca_{1-x}Eu_xB_6$ series suggested that the crystal symmetry may be lower than cubic [20].

The purpose of this work is to find a possible symmetry breaking in the crystal structure of EuB_6 that could explain the appearance of the FM ordering reported. For this reason we carefully studied the polarization and temperature dependence of the Raman scattering (RS) spectra of EuB_6 single crystals and performed *ab initio* calculations.

2. Experimental details

Single-crystalline samples of EuB_6 were grown in a flux of 99.999% pure Al, using the starting elements of Eu and B with purities of 99.95% and 99.99%, respectively [6]. Magnetic and transport characterization data can be found in [20]. The crystal's shapes were plate-like with typical dimensions of $0.5 \times 4 \times 6$ mm^3. Raman measurements were carried out using a triple spectrometer equipped with a LN_2 CCD detector. Each spectrum was corrected by the spectrometer response obtained by measuring the emission of a tungsten lamp and comparing it with the emissivity of a black body at the same temperature. The 514.5 nm line of an Ar^+ ion laser was used as the excitation source. The laser power was kept below 12 mW on a spot of diameter of about 100 μm. All measurements were made in a near-backscattering configuration.

For the cubic O_h RB_6 unit cell, the zone-center T_{2g}, E_g, and A_{1g} phonons are Raman active. These modes correspond to internal displacement of B atoms in the B_6 octahedron [21]. Previous RS works [21–29] have reported these modes at ~780 (T_{2g}), ~1150 (E_g), and ~1260 (A_{1g}) cm^{-1}. Besides these phonons, additional modes at ~200 and ~1400 cm^{-1} were also reported. The former was conclusively assigned to two-phonon RS [26] and the latter has had no clear assignment yet.

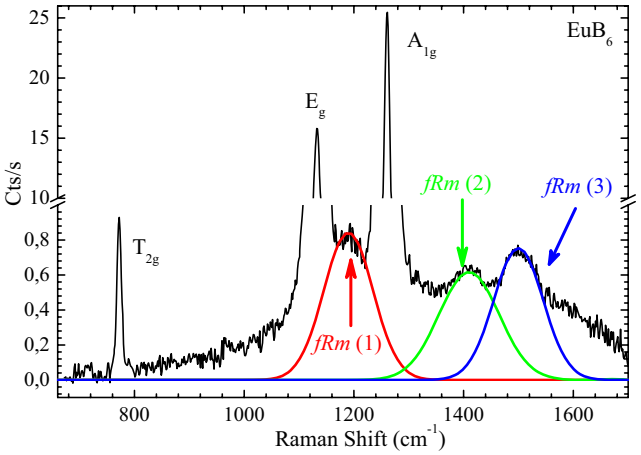

Figure 1. Room temperature unpolarized RS of EuB_6, showing the expected phonons of the O_h cubic structure as well as the forbidden ones.

(This figure is in colour only in the electronic version)

3. Results and discussion

Figure 1 presents the EuB_6 RS spectrum taken at 300 K. It shows the T_{2g}, E_g, and A_{1g} phonons of the cubic phase at 775, 1137 and 1264 cm^{-1}, respectively. Also, extra broad modes at ~1170, ~1400, and ~1500 cm^{-1} were observed. To verify the phononic origin of these extra modes we used another laser line (488.0 nm) to excite the sample. All modes were observed at the same Raman shift. The spectral intensity response was five times larger when the excitation was the 514.5 nm, indicating a possible resonant behavior. We shall label these extra modes as forbidden Raman modes fRm(1), fRm(2), and fRm(3), respectively. The other compounds of the $Ca_{1-x}Eu_xB_6$ series showed similar spectra. The intensity of the fRms appeared larger for $x = 0.10$.

For $x = 1$ and $x \geqslant 0.30$ a shoulder close to the E_g phonon was observed (not shown). This shoulder was always ~25 cm^{-1} above the E_g phonon frequency. For CaB_6 and EuB_6 it was attributed to the charge imbalance arising in the boron octahedron [21, 22, 27]. It is worth mentioning that the E_g peak had a symmetric shape for $x = 0.05$ and 0.10.

The polarized RS experiments were performed on the ab and ac planes at room T (figure 2). The a, b and c axes correspond to the [001], [010], and [100] crystallographic cubic directions [6]. The smaller crystal thickness determines the c axis (see the inset of figure 2(b)). The expected selection rules are summarized in table 1. It was found that A_{1g}, E_g, and T_{2g} phonons had the expected selection rules for the O_h space group. Analysis concerning the fRms is shown in table 2. Thus, the fRm(1) has a cubic A_{1g} symmetry. Instead, fRm(2) and fRm(3) did not appear on the T_{2g} channel probed with the (a, b) configuration (figure 2(b)) but were clearly observed on the same channel in the (c, a) case (figure 2(d)). Thus, we concluded that the symmetry of fRm(2) and fRm(3) is A, of a non-cubic group. The above, is strong evidence of an incipient breaking of the cubic symmetry. It is possible to consider that:

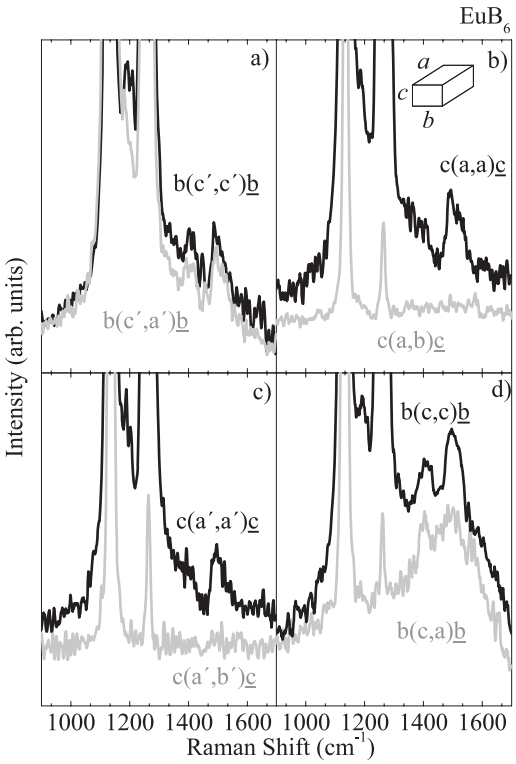

Figure 2. Room temperature polarized RS spectra for EuB_6 in the configurations listed in table 1. The inset of (b) shows the typical crystal shape and the a, b and c axes.

Table 1. Polarization selection rules in the O_h space group.

Configuration	Irreducible representation
a, b	T_{2g}
a, a	$A_{1g} + E_g$
a', a'	$A_{1g} + E_g + T_{2g}$
a', b'	$A_{1g} + E_g$
c, a	T_{2g}
c, c	$A_{1g} + E_g$
c', c'	$A_{1g} + E_g + T_{2g}$
c', a'	$E_g + T_{2g}$

(i) the fRm(1) is a doublet of the A_{1g} phonon originating from the charge imbalance arising in the B_6 octahedron, resembling the E_g doublet, and
(ii) the fRm(2) and fRm(3) are bands activated by the subtle non-cubic symmetry of the lattice.

The temperature dependence of the RS spectra is displayed in figure 3. The fRm(1) kept its intensity almost constant while the fRm(2) and fRm(3) modes presented a strong intensity increase at low temperatures, $T \lesssim 20$ K. The total integrated area of fRm(2) and fRm(3) increased nearly 6 times between 400 and 14 K. For $T > 400$ K, the peak's intensities were nearly constant.

Ogita *et al* [27] observed a broad peak at $\sim$1400 cm^{-1}, probably due to the superposition of fRm(2) and fRm(3) bands. These authors assigned it to an overtone of the T_{2g} phonon. This interpretation is incorrect for the following reasons: (i) the energy of this broad mode is smaller than twice the T_{2g} phonon frequency; (ii) the selection rule for this mode is incompatible with any combination of the O_h irreducible representations (IR), contrary to what was expected from the direct product $T_{2g} \bigotimes T_{2g} = A_{1g} + E_g + T_{1g} + T_{2g}$ [30]; and (iii) the temperature dependence is incompatible with a two-phonon RS process. These authors also observed a low frequency mode at $\sim$200 cm^{-1}, in agreement with other authors [22, 25, 26]. Since this mode was conclusively assigned to two-phonon RS [25] its selection rules will not be explored in this work.

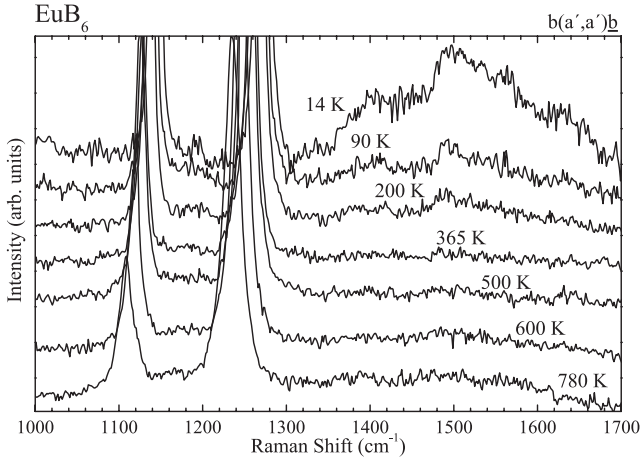

Figure 3. Temperature dependence of the RS spectra at a', a' polarization.

Table 2. Experimentally observed selection rules for the fRms.

	fRm(1)	fRm(2)	fRm(3)
$A_{1g} + E_g + T_{2g}$	×	×	×
$A_{1g} + E_g$	×	×	×
T_{2g} (a, b)	—	—	—
$E_g + T_{2g}$	—	—	—
T_{2g} (c, a)	—	×	×

Another scenario corresponds to considering the fRms as disorder-activated infrared-active phonons or combinations of Raman-active and infrared-active modes. Yahia *et al* [23] measured the RS and infrared reflectivity for several hexaborides. Comparing the frequencies of their infrared-active modes with the frequencies of the fRms, one concludes that there are no infrared modes, or possible combinations, that could be assigned to the fRm peaks. Thus, this assumption should also be disregarded. The cubic symmetry breaking proposed here is the straightforward scenario.

Notice that the A_{1g}, E_g, T_{2g} and fRm(1) phonons still have cubic symmetry. This suggests that the overall crystal distortion may be very small, which explains the difficulties of bulk techniques that explains x-ray diffraction studies in resolving large scale subtle symmetry changes.

Currently, high resolution synchrotron x-ray diffraction experiments (see, e.g., the work of Yang and Ren [31]) have shown that typical cubic ferromagnets like $DyCo_2$, $CoFe_2O_4$, and Terfenol-D experience a tiny structural change ($(c - a)/a \lesssim -1.0 \times 10^{-3}$) to a non-cubic symmetry at T_C. A similar subtle deviation of the cubic structure is probably appearing in

the hexaborides. However, the results presented here show that the crystallographic structure is non-cubic in the 14 and 780 K probed ranges. The intensity increase of fRm(2) + fRm(3) below 20 K is probably related to the enhancement of the $(c - a)/a$ ratio near to the magnetic transition driven by magnetoelastic coupling. This symmetry breaking may also allow the FM in this system.

We also performed spin-polarized first-principles calculations to corroborate these findings. Calculations were based on the all-electron projector augmented wave (PAW) method and density functional theory (DFT) within the local density approximation as implemented in VASP [32, 33]. Similar computational calculation methodology was recently employed by Kim *et al* [34] to successfully explain the optical conductivity of EuB_6.

In order to get the correct correlation among spin orientations and crystal structure optimization, the spin–orbit coupling was taken into account in a fully self-consistent way. The structural equilibrium volume for the [111] and [100] spin orientations was obtained by optimizing the internal forces and stress without taking the symmetry into account, i.e., all possible cell shapes were allowed. An energy cutoff of 500 eV was employed. A $(10 \times 10 \times 10)$ grid yielding 1000 **k**-points was used for the Brillouin zone interaction. Due to the small energy differences between spin orientations, the energy and force convergence criteria were set to 1×10^{-6} eV and 0.01 eV/Å, respectively. We have also performed LDA + U calculations [35]. As the Eu f levels are very localized, the results obtained with LDA + U were almost the same without the U parameters. Thus, in the following, only the LDA results will be presented.

It was found that the [111] spin configuration is 3.2 meV/EuB_6 lower in energy than the [100] one, in agreement with the magnetic characterization data from the literature [7].

In all cases, a small lattice distortion along the spin direction was observed. Although small, it was enough to break the cubic symmetry of the unit cell, allowing the occurrence of FM. For the Eu spin in the [111] direction, the unit cell lattice vectors obtained were

$$\vec{a} = 4.134\,43\hat{x} + 0.001\,24\hat{y} + 0.001\,24\hat{z};$$

$$\vec{b} = 0.001\,24\hat{x} + 4.134\,43\hat{y} + 0.001\,24\hat{z};$$

$$\vec{c} = 0.001\,24\hat{x} + 0.001\,24\hat{y} + 4.134\,43\hat{z}.$$

The resulting non-cubic unit cell had the boron octahedra slightly distorted in the spin direction. The values obtained for the lattice parameters are in excellent agreement with experimental findings (agreement better than 1.5%).

The [100] spin orientation leads to a slightly non-cubic structure of tetrahedral symmetry, i.e., $\vec{a} \neq \vec{b} = \vec{c}$. The optimized lattice vectors were

$$\vec{a} = 4.121\,78\hat{x}; \qquad \vec{b} = 4.121\,71\hat{y}; \qquad \vec{c} = 4.121\,71\hat{z}.$$

Furthermore, a distortion in the boron octahedron structure was also observed. For example, the u parameter, defined as the distance between the center of the unit cell and the B atoms, is smaller in the [100] direction than in the others: $u_{100} = 1.2350$ Å and $u_{010} = u_{001} = 1.2351$ Å. Although small ($\sim 1\times10^{-4}$ Å), these distortions were consistent with the lower symmetry observed by means of Raman scattering.

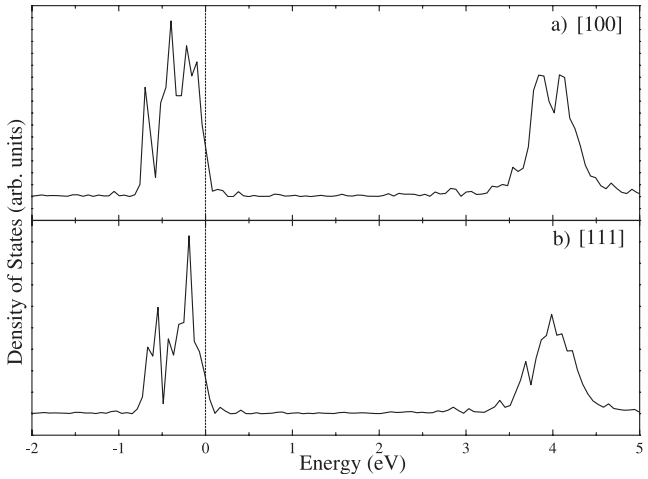

Figure 4. Local density of states (Eu f-states) for atomic displacements along the [100] (a) and [111] (b) directions.

The local magnetic moments, the shape of the Eu f wavefunction and the local density of states for the two configurations were very similar, and almost spin orientation independent. Figure 4 shows the projected density of states (DOS) relative to the Eu f levels for the two spin directions with magnetization along [100] (upper panel) and [111] (lower panel) directions. The DOS are very similar, with an exchange splitting of 4–5 eV. The dashed lines indicate the Fermi level. The most noticeable difference concerns the level splitting. Along the magnetization direction with the highest crystal symmetry ([111]) the levels are sharper than the tetragonal one ([100]). The [100] direction appeared more delocalized and had more peaks. That is probably due to crystal electric field effects. The computational simulations clearly show that the unit cell symmetry should be non-cubic in both configurations, in order to enable a net magnetic moment to be present in the unit cell.

4. Conclusions

In conclusion, the experimental results showed the appearance of three fRms in EuB_6 that do not belong to the expected set of Raman-active phonons of the O_h cubic group. After analyzing different possibilities it was concluded that fRm(1) is a doublet of the A_{1g} phonon, caused by a charge imbalance in the B_6 octahedron, similar to the E_g doublet. Also, the fRm(2) and fRm(3) bands arise from the cubic symmetry breaking that induces a non-cubic environment in the B_6 octahedron. First-principles calculations of magnetic and structural properties corroborated this symmetry breaking.

Acknowledgments

This work was supported by the Brazilian Agencies CNPq and FAPESP. SBO was partially supported by Raices 2009, Argentina.

References

[1] Etourneau J and Hagenmuller P 1985 *Phil. Mag.* B **52** 589
[2] Rhyee J-S, Oh B H, Cho B K, Kim H C and Jung M H 2003 *Phys. Rev.* B **67** 212407
[3] Paschen S, Pushin D, Schlatter M, Vonlanthen P, Ott H R, Young D P and Fisk Z 2000 *Phys. Rev.* B **61** 4174
[4] Caimi G, Broderick S, Ott H R, Degiorgi L, Bianchi A D and Fisk Z 2004 *Phys. Rev.* B **69** 12406
[5] Pereira V M, Lopes dos Santos J M B, Castro E V and Castro Neto A H 2004 *Phys. Rev. Lett.* **93** 147202
[6] Fisk Z, Johnston D C, Cornut B, von Molnar S, Oseroff S and Calvo R 1979 *J. Appl. Phys.* **50** 1911
[7] Süllow S, Prasad I, Aronson M C, Sarrao J L, Fisk Z, Hristova D, Lacerda A H, Hundley M F, Vigliante A and Gibbs D 1998 *Phys. Rev.* B **57** 5860
[8] Yu U and Min B I 2005 *Phys. Rev. Lett.* **94** 117202
[9] Zhang X, von Molnár S, Fisk Z and Xiong P 2008 *Phys. Rev. Lett.* **100** 167001
[10] Lin C and Millis A J 2005 *Phys. Rev.* B **71** 075111
[11] Degiorgi L, Felder E, Ott H R, Sarrao J L and Fisk Z 1997 *Phys. Rev. Lett.* **79** 5134
[12] Henggeler W, Ott H-R, Young D P and Fisk Z 1998 *Solid State Commun.* **108** 929
[13] Degiorgi L, Felder E, Ott H R, Sarrao J L and Fisk Z 1997 *Phys. Rev. Lett.* **79** 5134
[14] Süllow S, Prasad I, Aronson M C, Bogdanovich S, Sarrao J L and Fisk Z 2000 *Phys. Rev.* B **62** 11626
[15] Brooks M L, Lancaster T, Blundell S J, Hayes W, Pratt F L and Fisk Z 2004 *Phys. Rev.* B **70** 020401
[16] Wigger G A, Wälti Ch, Ott H R, Bianchi A D and Fisk Z 2002 *Phys. Rev.* B **66** 212410
[17] Wigger G A, Beeli C, Felder E, Ott H R, Bianchi A D and Fisk Z 2004 *Phys. Rev. Lett.* **93** 147203
[18] Urbano R R, Pagliuso P G, Rettori C, Schlottmann P, Sarrao J L, Bianchi A, Nakatsuji S and Fisk Z 2005 *Phys. Rev.* B **71** 184422
[19] Opechowski W and Guccione R 1965 *Magnetism* vol IIa, ed G T Rado and H Suhl (New York: Academic)
[20] Urbano R R, Pagliuso P G, Rettori C, Schlottmann P, Fisk Z and Oseroff S B 2006 *J. Appl. Phys.* **99** 08P701
[21] Udagawa M, Nagai S, Ogita N, Iga F, Kaji R, Sumida K, Akimitsu J, Kunii S, Suzuki K, Onodera H and Yamaguchi Y 2002 *J. Phys. Soc. Japan* **71** 314
[22] Mörke I, Dvorák V and Wachter P 1981 *Solid State Commun.* **40** 331
[23] Yahia Z, Turrell S, Mercurio J-P and Turrell G 1993 *J. Raman Spectrosc.* **24** 207
[24] Lemmens P, Hoffmann A, Mishchenko A S, Talantov M Yu and Güntherodt G 1995 *Physica* B **206/207** 371
[25] Nyhus P, Cooper S L, Fisk Z and Sarrao J 1995 *Phys. Rev.* B **52** R14308
[26] Nyhus P, Cooper S L, Fisk Z and Sarrao J 1997 *Phys. Rev.* B **55** 12488
[27] Ogita N, Nagai S, Okamoto N, Udagawa M, Iga F, Sera M, Akimitsu J and Kunii S 2003 *Phys. Rev.* B **68** 224305
[28] Teredesai P, Muthu D V S, Chandrabhas N, Meenakshi S, Vijayakumar V, Modak P, Rao R S, Godwal B K, Sikka S K and Sood A K 2004 *Solid State Commun.* **129** 791
[29] Song M, Yang I-S, Seo C W, Cheong H, Kim J Y and Cho B K 2007 *J. Magn. Magn. Mater.* **310** 1019
[30] Koster G F, Dimmock J O, Wheeler R G and Statz H 1963 *Properties of the Thirty-Two Point Groups* (Cambridge, MA: MIT Press)
[31] Yang S and Ren X 2008 *Phys. Rev.* B **77** 014407
[32] Kresse G and Hafner J 1993 *Phys. Rev.* B **47** R558
[33] Kresse G and Joubert D 1999 *Phys. Rev.* B **59** 1758
[34] Kim J, Kim Y-J, Kuneš J, Cho B K and Choi E J 2008 *Phys. Rev.* B **78** 165120
[35] da Silva J L F, Ganduglia-Pirovano M V and Sauer J 2007 *Phys. Rev.* B **76** 125117